

Magnetostratigraphy of the Yaha section, Tarim Basin (China): 11 Ma acceleration in erosion and uplift of the Tian Shan mountains

Julien Charreau : Institut des Sciences de la Terre d'Orléans; Bâtiment Géosciences, BP 6759, 45067 Orléans Cedex 2, France

Stuart Gilder : Laboratoire de Paléomagnétisme, Institut de Physique du Globe de Paris, 4 place Jussieu, 75252 Paris Cedex 05, France

Yan Chen : Institut des Sciences de la Terre d'Orléans, Bâtiment Géosciences, BP 6759, 45067 Orléans Cedex 2, France

Stéphane Dominguez : Laboratoire Dynamique de la Lithosphère, UMR Centre National de la Recherche Scientifique 5573, 22 Place Bataillon, 34095 Montpellier Cedex, France

Jean-Philippe Avouac : Division of Geological and Planetary Sciences, California Institute of Technology, Mail Code 100-23, Pasadena, California 91125, USA

Sevket Sen : Museum of Natural History, 43 rue Buffon, 75005 Paris Cedex 5, France

Marc Jolivet : Laboratoire Dynamique de la Lithosphère, UMR Centre National de la Recherche Scientifique 5573, 22 Place Bataillon, 34095 Montpellier Cedex, France

Yongan Li : Institute of Geology and Mineral Resources, Urumqi 83000, People's Republic of China

Weiming Wang : Nanjing Institute of Geology and Palaeontology, Chinese Academy of Sciences, 39 East Beijing Road, Nanjing 210008, People's Republic of China

Keywords: Tian Shan, uplift, erosion, magnetostratigraphy, Tarim.

ABSTRACT

We report a magnetostratigraphic and rock magnetic study of the Yaha section, located on the southern flank of the central Tian Shan mountains, Asia. Our results show a two-fold increase in sedimentation rate as well as marked changes in rock magnetic characteristics ca. 11 Ma. After 11 Ma, sedimentation rate remained remarkably constant until at least 5.2 Ma. These findings are consistent with sedimentary records from other sections surrounding the Tian Shan. We conclude that uplift and erosion of the Tian Shan accelerated ca. 11 Ma, long after the onset of the collision between India and Asia, and that the range rapidly evolved toward a steady-state geometry via a balance between tectonic and erosion processes.

INTRODUCTION

The Tian Shan range is among Asia's largest mountain chain, with summits higher than 7000 m dominating the landscape over an east-west distance of 2500 km (Fig. 1A). The range's geologic record attests to a complex history of Paleozoic subduction-related processes (Burtman, 1975; Windley et al., 1990), and a new phase of Cenozoic reactivation induced by the India-Asia collision (Tapponnier and Molnar, 1977). The exact timing of reactivation is poorly constrained, which inhibits a better understanding of the evolution of continental deformation due to an indenting India. In addition, the Tian Shan is a case example of an active intracontinental mountain belt where the history of mountain building might be deciphered from the sediment accumulation in the adjacent Tarim and Junggar Basins.

By comparing cumulative crustal shortening across the Tian Shan with current deformation rates, Avouac et al. (1993) estimated that the initiation of the deformation began at $16 \pm 22/-9$ Ma. Sedimentary logs of six deep drill cores from the basins surrounding the Tian Shan indicate that sediment flux accelerated after ca. 17 Ma (Métivier and Gaudemer, 1997). These estimates are consistent with in situ apatite fission-track analyses from sediments exposed both north and south of Tian Shan that suggest that unroofing began ca. 24–25 Ma (Hendrix et al., 1994; Dumitru et al., 2001). Younger exhumation ages of 13.6 ± 2.2 (1σ) and 13.1 ± 2.2 Ma are also recorded in the sediments from the Tarim Basin, south of the Tian Shan (Sobel and Dumitru, 1997). Magnetostratigraphic and geochronologic data from the Chu Basin in the western Kyrgyz Tian Shan suggest an increase in sedimentation rate by ca. 11 Ma (Bullen et al., 2001, 2003); a study of the Kuitun section shows that reactivation of the northern Tian Shan started before 10 Ma (Charreau et al., 2005). Reactivation ca. 10 Ma is consistent with extrapolating back in time the current rates of shortening across the range to explain cumulated shortening (Abdrakhmatov et al., 1996; Reigber et al., 2001).

Despite the growing number of observations, details about how and when the Tian Shan mountains were built remain vague, so we performed a magnetostratigraphic and rock magnetic study of the Yaha section, located on the southern flank of the Tian Shan mountains. This allows us to track changes in the sedimentation rate and the magnetic properties of the sediments through time, giving insight into the late Cenozoic erosion history of the Tian Shan.

GEOLOGICAL SETTING AND SAMPLING

The Yaha section is located near Kuche city, where the south-flowing Yaha River cuts the Qiulitage anticline (Fig. 1B). Seismic imaging by Suppe (2004, personal commun.) defined the fold as a 225-km-long active ramp anticline. The sampled section spans 2814 m in thickness (Figs. 1C, 1D), beginning ~200 m north of the Qiulitage fold axis, where 1069 paleomagnetic cores were drilled then oriented with magnetic and sun compasses. Two cores per horizon were collected with an average distance between horizons of 5.6 m. Each sampling layer was located to within a few centimeters using a differential global positioning system. The sediments at the base of the section are dominated by dark red muddy sandstone intercalated with siltstone and green-gray sandstone. The series becomes progressively coarser grained toward the top, until reaching a thick gray conglomerate unit, which likely belongs to the Xiyu Formation. Despite the presence of several small (<1 m offset) north-verging back thrusts, the section contains no significant duplication or any sign of major discordance, suggesting that sedimentation was relatively continuous. From the base to the top of the section, Yaha sediments are mapped as the Neogene Jidike, Kangcun, and Kuqa Formations (Geological and Mineral Resources Bureau of Xinjiang Uygur Autonomous Region, 1993.), yet the assigned age is based entirely on facies correlation. Although we found no vertebrate fossils, the spore and pollen compositions of two samples contain *Artemisiaepollenites* (*Artemisia*), probably indicating a middle Miocene to recent age.

ROCK MAGNETISM AND MAGNETOSTRATIGRAPHY

Curie point analyses show a rapid drop in magnetic susceptibility near 580 °C, followed by a progressive decrease in susceptibility until 680 °C, signaling the presence of both magnetite and hematite (GSA Data Repository Fig. DR1). Following pilot alternating field and thermal demagnetization experiments, thermal demagnetization was found to better isolate linear magnetization components. Most samples have two components; one at low temperatures (<300 °C) that is north and downward-directed in in situ coordinates and does not decay toward the origin on orthogonal diagrams, and another at high temperatures (300–680 °C) that is of dual polarity and decays toward the origin (Fig. DR2).

Of the 486 samples we demagnetized, 410 have high-temperature components (Table DR1), 13 have unstable magnetizations, and 63 have remanent directions that follow great circle trajectories, never defining a stable end point. We also collected and demagnetized 28 samples from 3 sites on the southern side of the anticline, and together with the samples from the magnetostratigraphic section, the fold test on the high-temperature component is positive at the 99% confidence level (McElhinny, 1964.) (Fig.

DR3). The mean inclination of normal polarity directions is 5.1° steeper than that of the reverse polarity directions; due to the extremely small uncertainties on both populations (α_{95} of 2.6° and 2.5° , respectively), this leads to a negative reversal test at the 95% confidence level (McFadden and McElhinny, 1990). Because the declinations are $\sim 180^\circ$ opposite (353.2° vs. 173.1°), the difference in inclination is likely due to a partially unremoved recent field magnetization, and we conclude that the high-temperature component represents a primary remanent magnetization.

A magnetostratigraphic sequence was established from samples having the high-temperature component determined from principal component analysis and whose directions are within 45° of the mean. These selection criteria, based on 388 samples, define 18 normal (1 to 18) and 17 reverse (a to q) polarity chrons (Figs. 2A–2C), each chron being defined by at least two samples from two different sedimentary horizons. We correlated the magnetostratigraphic sequence to the Berggren et al. (1995) reference scale (Fig. 2D) using the following criteria: (1) the high number of reversals is indicative of the middle to upper Tertiary; (2) *Artemisiaepollenites* likely suggests a Miocene or younger age; (3) there are five chrons, three reversed (a, d, and i) and two normal (8 and 14), of relatively long duration (>200 m thick); and (4) the top of the section is below the Pliocene–Pleistocene Xiyu Formation.

Figure 2C represents our preferred correlation, which provides the best available fit in terms of interval number and duration. There are problems in correlation between normal chrons 2 and 4, where a few short-duration polarity events are absent on the reference scale, and between normal chrons 14 and 15, where reversed event C5r.1n is missing. Despite these few incompatibilities, the correlation appears robust and limits the sampled sediments in time to 12.6 to 5.2 Ma. The nondecompacted sedimentation rate accelerates markedly between 10 and 11 Ma, with an average rate of 0.20 ± 0.07 mm/yr from 12.6 to ca. 11 Ma, which then doubles to 0.43 ± 0.16 mm/yr from ca. 10 Ma to the top of the section at 5.2 Ma (Figs. 2D and 3A). After decompaction, average sedimentation rates are 0.29 ± 0.10 mm/yr from 12.6 to ca. 11 Ma, and 0.53 ± 0.18 mm/yr from ca. 10 Ma to the top of the section at 5.2 Ma.

Figure 3B plots bulk magnetic susceptibility (κ) as a function of depth and time, where κ ranges from 100 to 550×10^{-6} SI (468 samples measured). Starting at the base of the section, κ drops from $\sim 500 \times 10^{-6}$ to $\sim 250 \times 10^{-6}$ by ca. 11 Ma. From 11 to 6.3 Ma, κ increases slowly and steadily to $\sim 300 \times 10^{-6}$. At 6.3 Ma, κ drops fairly quickly, and although the mean is relatively low, there are high-amplitude, short-frequency variations. We also analyzed 468 samples for anisotropy of magnetic susceptibility (AMS). The mean shape of the anisotropy ellipsoid, called the T parameter (Hrouda, 1982), is plotted in Figure 3C as a function of depth. Important changes are observed between 11.2 and 10.7 Ma, with T signaling a change from relatively spherical ($T \approx 0$) to

distinctly oblate ($T > 0$) shapes. The change in T ca. 11 Ma does not coincide with changes in κ or the percentage of anisotropy (P') (Fig. 3D).

IMPLICATIONS FOR THE EROSION HISTORY AND GROWTH OF THE TIAN SHAN MOUNTAINS

Our magnetostratigraphic and rock magnetic study of the Yaha section dates the sampled section between 12.6 and 5.2 Ma. During that time: (1) sedimentation rate doubled ca. 11 Ma, (2) average grain shape went from spherical to oblate ca. 11 Ma, and (3) long-term magnetic susceptibility trends occur near the bottom of the section and ca. 6 Ma. The AMS T parameter can yield information related to the hydrologic regime and transport conditions of the sediments when the sedimentary fabric has not been significantly overprinted by compaction or tectonic-related processes (Gilder et al., 2001; Charreau et al., 2005). This would not be the case if P' and/or κ underwent changes that correlate with T . If P' was dominated by a postsedimentation fabric, e.g., due to compaction, P' should increase and T should become more oblate as a function of depth; neither of these are observed at Yaha. Moreover, no significant change in lithology is observed where the T parameter changes and the sedimentation rate increases. Thus it seems that the departure from spherical to oblate values is related to how the particles were oriented during deposition or to differences in the particle shapes. When T is near 0, the particles were likely transported far enough that they became sufficiently eroded to be spherical on average, or they were deposited in an environment where they acquired no systematic preferred orientation. Viewed at a single profile in a basin, the significant change in T from spherical before 11 Ma to distinctly oblate after 11 Ma (Fig. 3) could be due to tectonism, via propagation of thrusting at the margins of the mountain, moving the mountain front closer to the deposition site; this reduces the distance traveled by the particles, and thus the amount they are eroded, and/or changes their hydrologic regime.

Because the Junggar and Tarim Basins are internally filled, the total sediment flux directly reflects the denudation rates over the Tian Shan and can thus indicate the topographic evolution of the range (Métivier and Gaudemer, 1997). The accelerated sedimentation rates ca. 11 Ma could then be translated as due to higher erosion rates from accelerated uplift. While sedimentation rates in the Kuche Basin could reflect the base-level history of the entire Tarim Basin, which also depend on sediments shed from the Kunlun and Pamir mountains, the morphology of the Tarim Basin suggests that the Tian Shan probably dominates the sedimentary flux delivered to the Kuche Basin. Moreover, as Métivier et al. (1999) pointed out, one-dimensional sedimentation rates should be viewed with caution, because the sedimentation rate at one point may not correlate with the total sediment flux delivered to the basin. However, because the Chu section exhibits a

significant increase in sedimentation rate ca. 11 Ma (Bullen et al., 2001, 2003), a more widespread (nonlocal) event on the Tian Shan is plausible.

Discriminating between tectonic and climatic forcing on changes in sedimentation rate is not straightforward (Molnar and England, 1990). Analog and numerical models suggest that mountain belts tend to an equilibrium state where the topography remains constant (Avouac and Burov, 1996; Willett et al., 2001; Lague et al., 2003; Babault et al., 2005). In numerical models, this equilibrium arises due to coupling between erosion, the thermal structure of the range, and deformation of the crust and lithosphere (Avouac and Burov, 1996; Cattin and Avouac, 2000). Under conditions of constant erosion, accelerated tectonic uplift via horizontal shortening results in mountain ranges with steeper topographies. Yet, as the range's surface progressively grows, sedimentation rates would continuously increase despite the constant erosion rates. At Yaha, the sedimentation rate appears more linear than exponential between ca. 11 Ma and 5.2 Ma, suggesting compensation by heightened erosion. Although there are no paleoenvironmental data for that time in this region, the presence of *lodes* in the ca. 7.5 Ma level of the Kuitun section indicates a hot and wet environment (this genus currently resides in the tropical regions of Africa, India, and Madagascar; Charreau et al., 2005).

When a change in climate drives an increase in erosion rate, uncompensated by a change in tectonic shortening, the topography of the range should decrease. Numerical simulations of this process, which account for isostatic compensation and viscous deformation of the lower crust and the upper mantle, indicate that the characteristic relaxation time for a mountain range the size of Tian Shan, with erosion rates consistent with the observed sediment flux, would be a few million years (Avouac and Burov, 1996). Our data do not show any such relaxation, suggesting that either the 5–6 m.y. time span is too short, or, more probably, that the increase in erosion flux was compensated by a coeval increase in crustal flux into the orogen. We thus propose that by ca. 11 Ma, the Tian Shan underwent a rapid transition to a regime with both higher tectonic uplift and erosion rates. However, because fission-track ages from various sections in the Tian Shan area show that the range was reactivated ca. 24 Ma (Hendrix et al., 1994; Sobel and Dumitru, 1997; Dumitru et al., 2001), the phase of amplified uplift and erosion at 11 Ma was likely not the sole event leading to the buildup of the modern Tian Shan.

ACKNOWLEDGMENTS

We dedicate this paper to Shaozhu Wu, whose unselfish and invaluable contributions will be sorely missed. We thank Ed Sobel, Rob Coe, John Suppe, and Neil Opdyke for their critical reviews. This study was financed by the French Institut National des Sciences de l'Univers program ECLISPE (Environnement et Climat du Passé: Histoire et Evolution) and the Chinese

project 2005CB422101. This is Institut de Physique du Globe de Paris contribution 2100.

REFERENCES CITED

Abdrakhmatov, K.Y., Aldazhanov, S.A., Hager, B.H., Hamburger, M.W., Herring, T.A., Kalabaev, K.B., Makarov, V.I., Molnar, P., Panasyuk, S.V., Prilepin, M.T., Reilinger, R.E., Sadybakasov, I.S., Souter, B.J., Trapeznikov, Y.A., Tsurkov, V.Y., and Zubovich, A.V., 1996, Relatively recent construction of the Tien Shan inferred from GPS measurements crustal deformation rates: *Nature*, 384, 450–453,.

Avouac, J.P., and Burov, E.B., 1996, Erosion as a driving mechanism of intracontinental mountain growth: *Journal of Geophysical Research*, 101, 17747–17769,.

Avouac, J.P., Tapponnier, P., Bai, P., You, M., and Wang, G.A., 1993, Active thrusting and folding along the northern Tien Shan and late Cenozoic rotation of the Tarim relative to Dzungaria and Kazakhstan: *Journal of Geophysical Research*, 98, 11791–11808.

Babault, J., Bonnet, S., Crave, A., and Van Den Driessche, J., 2005, Influence of piedmont sedimentation on erosion dynamics of an uplifting landscape: An experimental approach: *Geological Society of America Bulletin*, 33, 301–304.

Berggren, W.A., Kent, D.V., Swisher, C.C., and Aubry, M.P., 1995, A revised geochronology and chronostratigraphy.: *in* Berggren, W.A., et al., eds., *Geochronology time scales and global stratigraphic correlation: SEPM (Society for Sedimentary Geology) Special Publication 54*, 210 p.

Bullen, M.E., Burbank, D.W., Garver, J.I., and Abdrakhmatov, K.Y., 2001, Late Cenozoic tectonic evolution of the northwestern Tien Shan: New age estimates for the initiation of mountain building: *Geological Society of America Bulletin*, 113, 1544–1559,. doi: 10.1130/0016-7606(2001)113<1544:LCTEOT>2.0.CO;2.

Bullen, M.E., Burbank, D.W., and Garver, J.I., 2003, Building the Northern Tien Shan: Integrated thermal, structural, and topographic constraints: *Journal of Geology*, 111, 149–165,. doi: 10.1086/ 345840.

Burtman, V.S., 1975, Structural geology of the Variscan Tian Shan, USSR: *American Journal of Science*, 275-A, 157–186.

Cattin, R., and Avouac, J.P., 2000, Modeling mountain building and the seismic cycle in the Himalaya of Nepal: *Journal of Geophysical Research*, 105, 13389–13407.

Charreau, J., Chen, Y., Gilder, S., Dominguez, S., Avouac, J.P., Sen, S., Sun, D.J., Li, Y.A., and Wang, M.W., 2005, Magnetostratigraphy and rock magnetism of the Neogene Kuitun He section (northwest China): Implications for late Cenozoic uplift of the Tianshan mountains: *Earth and Planetary Science Letters*, 230, 177–192,.

Dumitru, T.A., Zhou, D., Chang, E.Z., Graham, S.A., Hendrix, M.S., Sobel, E.R., and Carroll, A.R., 2001, Uplift, exhumation, and deformation in the Chinese Tian Shan,: *in* Hendrix, M.S., and Davis, G.A., eds., *Paleozoic and Mesozoic tectonic evolution of central Asia: From continental assembly to intracontinental deformation: Geological Society of America Memoir 194*, p. 71–99.

Geological and Mineral Resources Bureau of Xinjiang Uygur Autonomous Region, , 1993, *Regional geology of Xinjiang Uygur Autonomous Region: Ministry of Geology and Mineral Resources of the People's Republic of China, Geological Memoirs*, v. 1, 841 p.

Gilder, S., Chen, Y., and Sen, S., 2001, Oligo-Miocene magnetostratigraphy and rock magnetism of the Xishuigou section, Subei (Gansu Province, western China) and implications for shallow inclinations in central Asia: *Journal of Geophysical Research*, 106, 30505–30521,.

Hendrix, M.S., Dumitru, T.A., and Graham, A.S., 1994, Late Oligocene–early Miocene unroofing in the Chinese Tian Shan: An early effect of the India-Asia collision: *Geology*, 22, 487–490

Hrouda, F., 1982, Magnetic anisotropy of rocks and its application in geology and geophysics: *Surveys in Geophysics*, 5, 37–82,.

Lague, D., Crave, A., and Davy, P., 2003, Laboratory experiments simulating the geomorphic response to tectonic uplift: *Journal of Geophysical Research*, v. 108, doi:10.1029/2002JB0011785, 11 p.

McElhinny, M.W., 1964, Statistical significance of the fold test in paleomagnetism: *Royal Astronomical Society Geophysical Journal*, 7, 457–468.

McFadden, P.L., and McElhinny, M.W., 1990, Classification of the reversal test in paleomagnetism: *Geophysical Journal International*, 103, 725–729.

Métivier, F., and Gaudemer, Y., 1997, Mass transfer between eastern Tien Shan and adjacent basins (central Asia): Constraints on regional tectonics: *Geophysical Journal International*, 128, 1–17.

Métivier, F., Gaudemer, Y., Tapponnier, P., and Michel, K., 1999, Mass accumulation rates in Asia during the Cenozoic: *Geophysical Journal International*, 137, 280–318.

Molnar, P., and England, P., 1990, Late Cenozoic uplift of mountain ranges and global climate change: Chicken or egg?: *Nature*, 346, 29–34,.

Reigber, C., Michel, G.W., Galas, R., Angermann, D., Klotz, J., Chen, J.Y., Papschev, A., Arslanov, R., Tzurkov, V.E., and Ishanov, M.C., 2001, New space geodetic constraints on the distribution of deformation in the Central Asia: *Earth and Planetary Science Letters*, 191, 157–165,.

Sobel, E.R., and Dumitru, T.A., 1997, Thrusting and exhumation around the margins of the western Tarim basin during India-Asia collision: *Journal of Geophysical Research*, 102, 5043–5063,.

Tapponnier, P., and Molnar, P., 1977, Active faulting and tectonics in China: *Journal of Geophysical Research*, 82, 2905–2930.

Willet, S.D., Slingerland, R., and Hovius, N., 2001, Uplift, shortening, and steady state topography in active mountain belts: *American Journal of Science*, 301, 455–485.

Windley, B.F., Allen, M.B., Zhang, C., Zhao, Z.Y., and Wang, G.R., 1990, Paleozoic accretion and Cenozoic deformation of the Chinese Tien Shan Range, central Asia: *Geology*, 18, 128–131

FIGURES

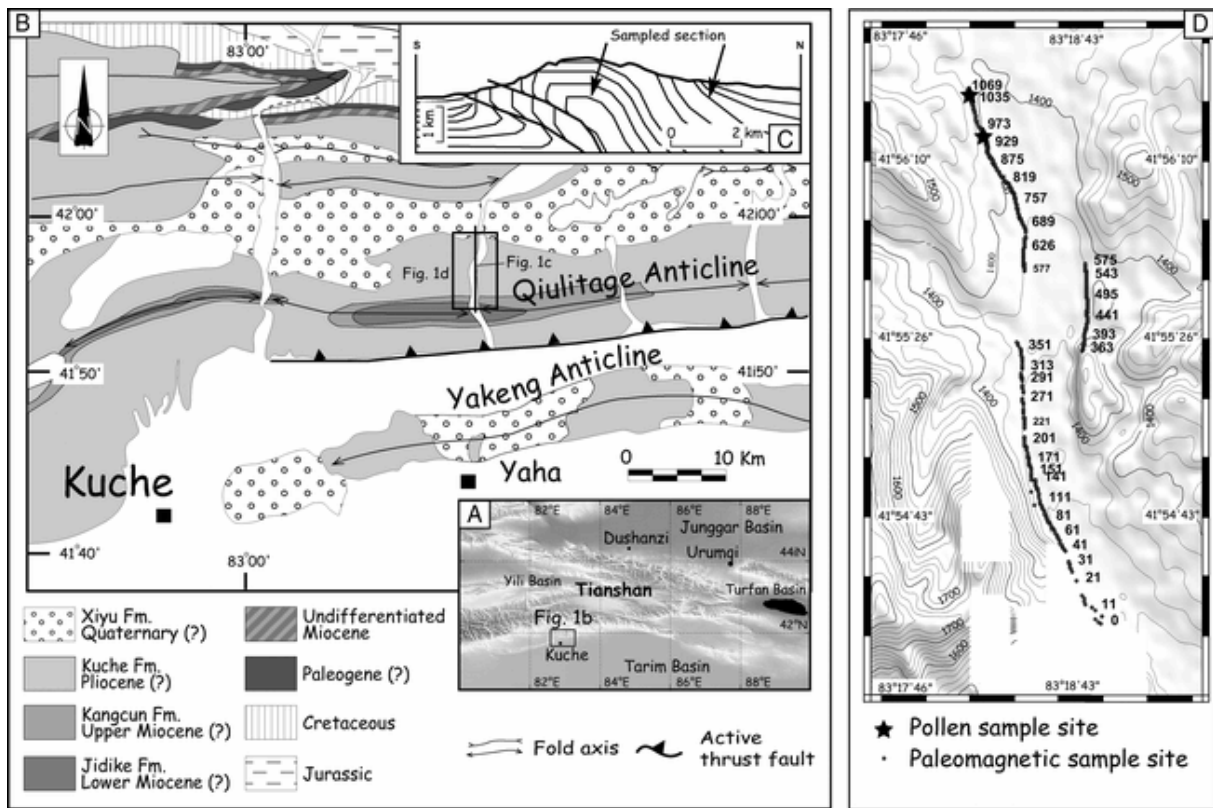


Figure 1. A: Topographic and locality map of central Asia. B: Geological map of Kuche area (after Geological and Mineral Resources Bureau of Xinjiang Uygur Autonomous Region, 1993). C: Cross section of Yaha River valley at Qiulitage anticline. D: Shuttle Radar Topography Mission (SRTM) digital elevation model along Yaha River showing paleomagnetic and pollen sample localities

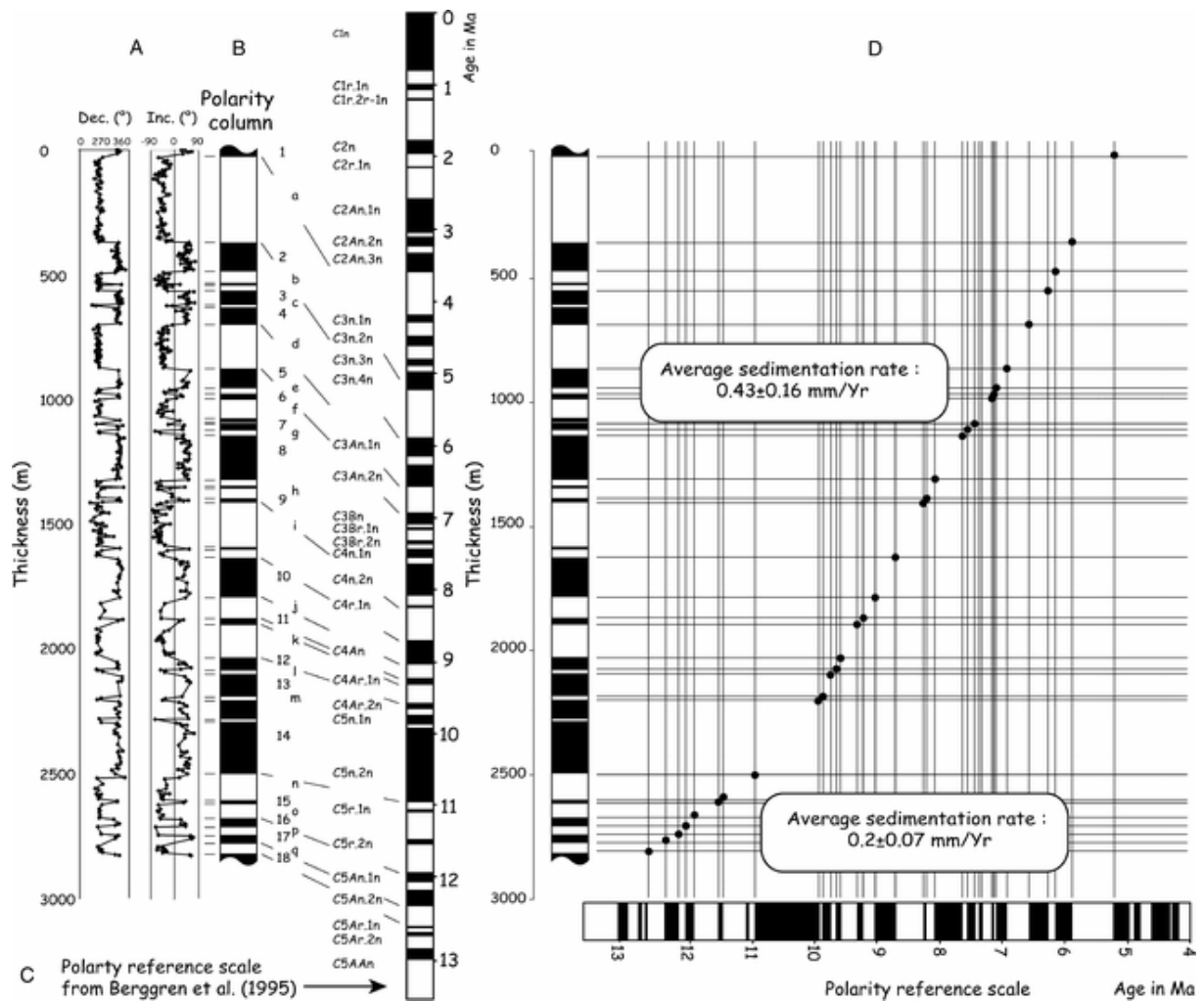


Figure 2. A: Magnetic declination (Dec.) and inclination (Inc.) corresponding to samples fit with principal component analysis. B: Magnetostratigraphic column from this study. Each normal (black) and reverse (white) polarity chron is defined by at least two samples from two different sedimentary horizons. Reversals found in single bed are shown in gray. C: Reference polarity time scale after Berggren et al. (1995). D: Age vs. depth plot of Yaha section, using data and correlation from B and C

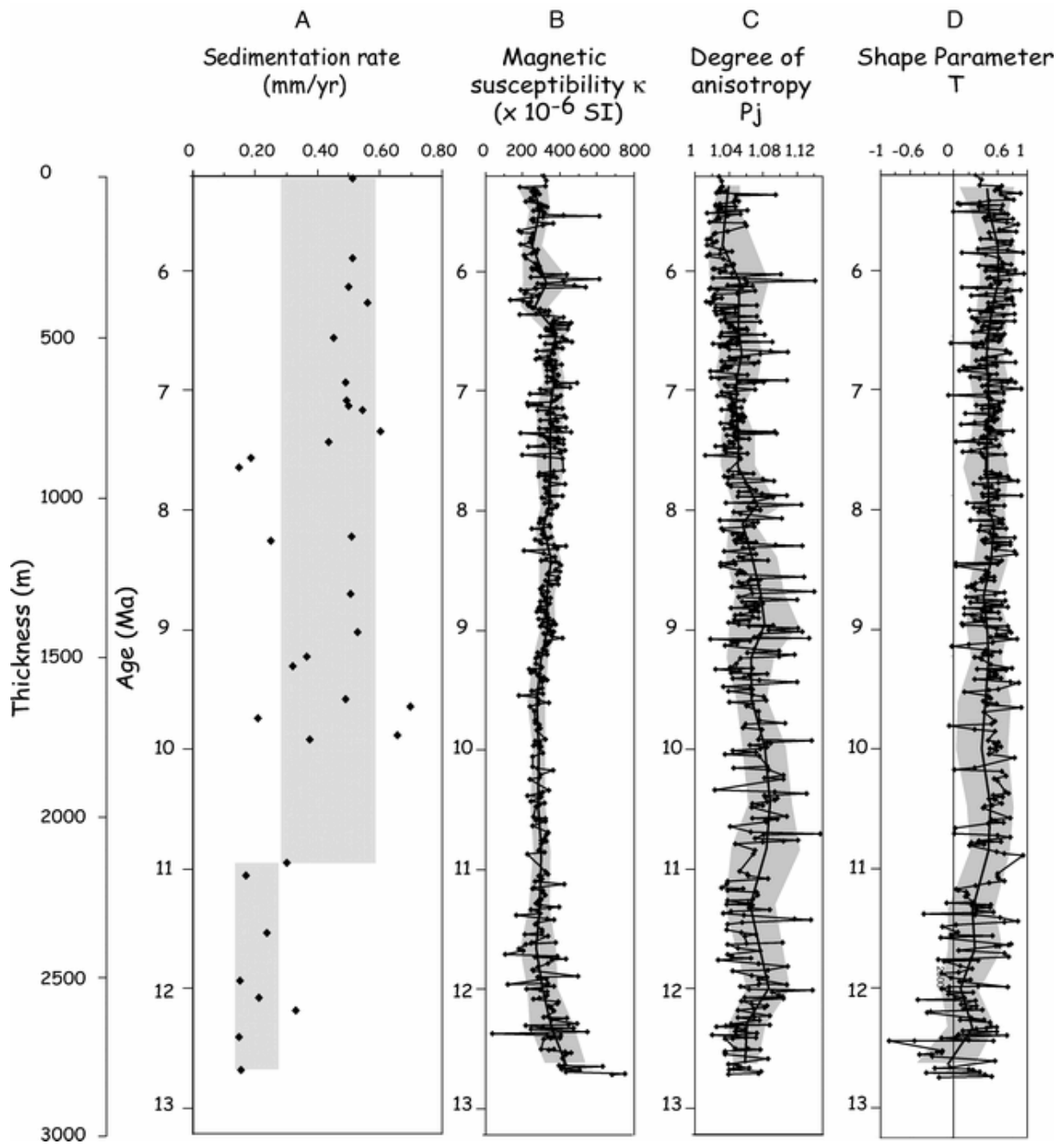


Figure 3. A: Plot of instantaneous sedimentation rate of data shown in [Figure 2D](#) (uncertainty envelope in gray). B: Magnetic susceptibility (κ), (C) magnetic anisotropy, and (D) shape parameter T as function of depth and time for Yaha section